TESTING FOR STRUCTURAL CHANGE IN AR(1) MODELS WITH WAVELETS

by

Xiangyu Zhang

M.A., Xiamen University, 2017
B.Sc., Jilin University, 2014

Thesis Submitted in Partial Fulfillment of the
Requirements for the Degree of
Master of Arts

in the
Department of Economics
Faculty of Arts and Social Sciences

SIMON FRASER UNIVERSITY
Spring 2019

APPROVAL

Name:	**Xiangyu Zhang**
Degree:	**Masters of Arts (Economics)**
Title of Thesis:	**Testing for Structural Change in AR(1) Models with Wavelets**
Examining Committee:	**Chair: Christoph Luelfesmann** Professor

Bertille Antoine
Senior Supervisor
Associate Professor

Alexander Karaivanov
Supervisor
Professor
Graduate Program Chair

Jean-François Bégin
External Examiner
Assistant Professor
Statistics and Actuarial Science
Simon Fraser University

Date Defended/Approved: April 11, 2019

Abstract

This paper develops a new procedure to test the changes in the autocorrelation structure of an AR(1) process by constructing a test statistic of cumulative sum (CUSUM) of squares based on a specific frequency decomposition of the variance using the maximal overlap discrete wavelet transformation (MODWT). The wavelet approach is appealing since it is based directly on the different behavior of the spectra of autoregressive processes with different coefficients. A feasible version of the test and the empirical quantiles of the test statistic are given. We demonstrate the size and power properties of the proposed test through Monte Carlo simulations.

Keywords: Structural Change; Serial Correlation; Autoregressive Model; Wavelets

Dedication

To my parents, Shengzhong and Xia.

Acknowledgements

I am indebt to the late Professor Ramazan (Ramo) Gençay, who introduced me to wavelets and their applications in economics and finance. As for me, Ramo was an encouraging, reliable and supportive advisor and friend. I will be ever grateful for his guidance, and am so sorry that he cannot see me graduate. I am very grateful to my supervisors Professor Bertille Antoine and Professor Alexander Karaivanov for their encouragement and kind, generous support. I appreciate a lot the time and effort they have spent on helping me.

I would like to acknowledge all my teachers in the MA program here in the Department of Economics for their generosity in sharing their knowledge.

I would also like to thank Professor Christoph Luelfesmann and Professor Jean-François Bégin for their service in the thesis examining committee.

Last but by no means least, I appreciate the generous help from the Department's administration team and support staff, especially Professor Alexander Karaivanov, Professor Brian Krauth, Ms. Lisa Agosti and Ms. Gwen Wild.

Table of Contents

[1]This chapter closely follows Percival and Walden (2000) and Gençay et al. (2001), where detailed treatments of wavelet transforms can be found.

Chapter 1

Introduction

The identification of structural changes (structural breaks) has become an integral part of many research fields in economics and finance (Perron, 2006). Various methods were first developed for independent observations. Later, some methods were extended to incorporate serial dependence of observations into consideration (Aue and Horváth, 2012). The goal of this thesis is to present a test that can be used to identify structural change at an unknown point in the autocorrelation coefficient of an AR(1) process.

This thesis contributes to the literature by providing a new direction for detection of structural change in the correlation structure. To be specific, the procedure proposed here for detection of structural change in an AR(1) model is based on a specific frequency decomposition of the variance using the wavelet transformation. The wavelet transformation can be used to decompose a time series into different sets of coefficients each associated with a certain time and a specific frequency band. We will give a brief introduction of the theory of wavelet transformation in the next chapter.

There is a large literature on tests of structural change. The celebrated Chow (1960) test was based on the F statistic for detection of structural change with known change points. Brown et al. (1975) proposed the cumulative sum (CUSUM) test based on recursive residuals for detection of structural change in regression coefficients with unknown change points. Ploberger and Krämer (1992) provided another implementation of the CUSUM test based on OLS residuals. Inclan and Tiao (1994) then proposed a procedure to detect variance changes in a sequence of independent observations based on the CUSUM of squares of the original series. Then Gombay and Serban (2009) extended the CUSUM test for detecting a change in the parameters of an autoregressive time series model based on large sample approximations to the efficient score vector under the null hypothesis of no change and the alternative hypothesis. More recently, Aue and Horváth (2012) provided a review on extensions of the CUSUM test to work for identification of structural changes in data with serial dependence. Apart from the detection of structural change, the estimation method for identifying the location of change points is also studied in the literature. Hinkley (1971) proposed an estimation method of change location in mean in a sequence of normal random variables based on a cumulative sum test scheme. Bai (1994, 1997) developed the least-square estimation method for the change location of a one-time change in a linear regression model. Bai and Perron (1998)

then extend the least-square estimation method to the case of multiple change points in a linear regression model.

Recently, the wavelet method has been used in developing statistical test. Fan and Gençay (2010) developed a wavelet approach to testing the presence of a unit root in a process based on a variance ratio test statistic. Gençay and Signori (2015) proposed a new family of tests for serial correlation using the wavelet transformation. Then, Li and Gençay (2017) extended the wavelet-based serial correlation test for observable series to unobserved error terms in a linear dynamic regression model. Wavelet methods have also been used in testing for the structural change in time series. Whitcher et al. (2002) applied the discrete wavelet transformation into testing the homogeneity of variance in a long memory series. And recently, Yazgan and Özkan (2015) proposed a wavelet method to identify structural changes in the mean of an independently distributed process.

In this thesis, we develop a test of structural change in the autocorrelation structure with cumulative sum (CUSUM) of squares based on a specific frequency decomposition of the variance using the maximal overlap discrete wavelet transformation (MODWT). Our test is then applied to the US inflation rate series.

The basic idea behind this test can be seen from the spectrum diagrams for AR(1) processes with different autocorrelation coefficients, which will be explained below. The power spectrum (or power spectral density) describes the distribution of the variance (power) of a certain time series (say, $y(t)$) over different frequency bands. It is defined as $S_y(f) = |\hat{y}(f)|^2$, where $\hat{y}(f) = \int_{-\infty}^{\infty} e^{-2\pi i f t} y(t)\, dt$ is the Fourier transform of the time series $y(t)$. It measures the contribution of the variance at a certain frequency band relative to the overall variance of the whole process. It is known that the spectrum of a unit root process is infinite at the origin, which means the variance of a unit root process is largely contributed by low frequencies (Fan and Gençay, 2010). The proportion in which the variance at a certain frequency band contributes to the overall variance of the whole process is associated with the serial correlation structure of the series. As the autocorrelation coefficient of a correlated series varies, the proportion in which the variance of a particular frequency band contributes to the variance of the whole process also changes in a certain pattern. Such a pattern is the basis of the test developed in this thesis.

Figure 1 in Appendix A shows several spectra for AR(1) processes with autocorrelation coefficients of -0.8, -0.4, 0, 0.4, 0.8 respectively. The pattern is clear that as the autocorrelation coefficient increases from a value close to -1 to a value close to 1, the proportion in which the variance of a particular frequency band, say, the low frequency band of $[0, 0.25]$, contributes to the variance of the whole process also increases gradually. This pattern motivates the testing method developed in this thesis.

To perform the test, we first decompose the original series into several series of coefficients each associated with changes in a certain frequency band (or scale) using the MODWT. [1] Then we

[1] We will give a brief introduction of the theory of wavelet transformation (including the discrete wavelet transformation (DWT) and the maximum overlap discrete wavelet transformation (MODWT)) in the next chapter.

construct the test statistic based on the CUSUM of squares of the scaling coefficients, which are associated with a (weighted) average over the low frequency band. Under the null hypothesis of no change in the autocorrelation coefficient, the statistic will oscillate around 0, while under the alternative, it will deviate from 0 and goes out of some specified boundary with a high probability. Given a data series, we fit an AR(1) model to the data based on the Yule-Walker method to estimate the autocorrelation coefficient under the null as well as the mean and standard error of the error terms. With these estimates, we propose a feasible version of the test statistic and get the empirical critical values through Monte Carlo simulations. And size and power properties of this test are demonstrated through Monte Carlo simulations.

The remainder of this thesis is organized as follows. In chapter 2, we report an overview of the wavelet theory needed in conducting the test proposed in this paper. In chapter 3, we first develop the test of no change in the autocorrelation structure of an AR(1) process against a change at some unknown point in sections 3.1 and 3.2. Then we demonstrate the size and power properties of the proposed test through Monte Carlo simulations in section 3.3. And, in section 3.4, we apply our test to the US inflation rate series. Finally, chapter 4 concludes.

Chapter 2

Wavelet Transformations[1]

The cumulative sum (CUSUM) of squares test statistic proposed here is based on a specific frequency decomposition of the variance, and we use the maximal overlap discrete wavelet transformation (MODWT) to get such a frequency decomposition. In this chapter, we will introduce the discrete wavelet transformation (DWT) and the MODWT.

As defined in Percival and Walden (2000), a wavelet is a small wave that grows and decays essentially in a limited time period. To quantify the notion, consider a real-valued function $\psi(\cdot)$ such that the integral of $\psi(\cdot)$ is zero, $\int_{-\infty}^{\infty}\psi(u)du = 0$, and the square of $\psi(\cdot)$ integrates to unity, $\int_{-\infty}^{\infty}\psi^2(u)du = 1$. Therefore, $\psi(\cdot)$ will make some excursions away from zero but any excursions above zero will be cancelled out by excursions below zero (Fan and Gençay, 2010). The two properties above lead to a wavelet function. Based on the wavelet functions, we can construct a filter that can be used to decompose a time series into coefficients associated with time and a specific frequency band (also called a scale).

There are many wavelet decompositions available in the literature. In the following, we start by introducing the discrete wavelet transformation (DWT), and then the maximum overlap discrete wavelet transformation (MODWT).

2.1 Discrete Wavelet Transformation (DWT)

The continuous wavelet function $\psi(\cdot)$ above has its discrete counterpart. Let $\{h_l : l = 0,\ldots,L-1\}$ be a real-valued discrete wavelet filter, where L is the width of the filter and should be an even number.[2] A wavelet filter must satisfies the following three properties:

$$\sum_{l=0}^{L-1} h_l = 0 \quad \text{(sum to zero);} \tag{2.1}$$

[1]This chapter closely follows Percival and Walden (2000) and Gençay et al. (2001), where detailed treatments of wavelet transforms can be found.

[2]Also called a high-pass filter.

$$\sum_{l=0}^{L-1} h_l^2 = 1 \quad \text{(unit energy)}; \tag{2.2}$$

and should be orthogonal to its even shifts:

$$\sum_{l=0}^{L-1} h_l h_{l+2n} = \sum_{l=-\infty}^{\infty} h_l h_{l+2n} = 0, \quad \text{for all nonzero integers } n. \tag{2.3}$$

A simple example of a wavelet filter is the Haar wavelet filter:[3]

$$\left\{ h_0 = \frac{1}{\sqrt{2}},\, h_1 = -\frac{1}{\sqrt{2}} \right\}. \tag{2.4}$$

Furthermore, we obtain the complementary to the wavelet filter, i.e., the scaling filter, $\{g_l : l = 0,\ldots,L-1\}$, by using the quadrature mirror relation:[4]

$$g_l \equiv (-1)^{l+1} h_{L-1-l}. \tag{2.5}$$

As an example, given the Haar wavelet filter defined above, the corresponding Haar scaling filter is:

$$\left\{ g_0 = -h_1 = \frac{1}{\sqrt{2}} \text{ and } g_1 = h_0 = \frac{1}{\sqrt{2}} \right\}. \tag{2.6}$$

By applying the wavelet filter and the scaling filter defined above to an observed time series, we can decompose the oscillations of that process into a high frequency part and a low frequency part. Let $\mathbf{y} = \{y_t\}_{t=0}^{T-1}$ be a vector of observations with dyadic length T, where $T = 2^J$, i.e., $J = \log_2(T)$. The vector of DWT coefficients $\mathbf{w}$ is obtained by:

$$\mathbf{w} = \mathscr{W}\mathbf{y}, \tag{2.7}$$

where $\mathscr{W}$ is a $T \times T$ real-valued orthonormal transformation matrix such that $\mathscr{W}^T\mathscr{W} = I_T$ (the $T \times T$ identity matrix). We express the DWT coefficients as a length $J+1$ vector:

$$\mathbf{w} = \left[\mathbf{w}_1, \mathbf{w}_2, \ldots, \mathbf{w}_J, \mathbf{v}_J\right]', \tag{2.8}$$

where $\mathbf{w}_j$ is a vector of length $T/2^j$ which is associated with changes on a scale of $\lambda_j = 2^{j-1}$, and $\mathbf{v}_J$ is a vector of length $T/2^J$ which is associated with averages on a scale of $2^J = 2 \cdot \lambda_J$.

In practice, a pyramid algorithm is used to compute the DWT. First, filter the data series $\mathbf{y}$ using the high-pass filter $\{h_l\}$ and the low-pass filter $\{g_l\}$ to obtain first level wavelet and scaling coefficients:

[3] It is equivalent to a Daubechies extremal phase wavelet filter of length $L = 2$, which is also denoted as the D(2) filter.

[4] Also called a low-pass filter.

$$W_{1,t} = \sum_{l=0}^{L-1} h_l y_{2t+1-l \bmod T} \quad \text{and} \quad V_{1,t} = \sum_{l=0}^{L-1} g_l y_{2t+1-l \bmod T}, \quad t = 0, 1, \ldots, \frac{T}{2} - 1, \tag{2.9}$$

where these $T/2$ wavelet coefficients and $T/2$ scaling coefficients form the vector of unit scale wavelet and scaling coefficients. We denote the first level partial DWT as $\mathbf{w} = \left[\mathbf{w}_1, \mathbf{v}_1\right]'$.

Next, we repeat the above filtering operations on the previous level scaling coefficient to obtain next level wavelet and scaling coefficients:

$$W_{j,t} = \sum_{l=0}^{L-1} h_l V_{j-1,2t+1-l \bmod (T/2^{j-1})} \quad \text{and} \quad V_{j,t} = \sum_{l=0}^{L-1} g_l V_{j-1,2t+1-l \bmod (T/2^{j-1})}, \quad t = 0, 1, \ldots, \frac{T}{2^j} - 1, \tag{2.10}$$

After repeating the above operations up to J times and keeping all vectors of wavelet coefficients and the final level (i.e., J-th level) scaling coefficients, we get the decomposition vector as defined above: $\mathbf{w} = \left[\mathbf{w}_1, \mathbf{w}_2, \ldots, \mathbf{w}_J, \mathbf{v}_J\right]'$.

The orthonormality of the transformation matrix $\mathscr{W}$ implies the variance preserving property of DWT:[5]

$$\|\mathbf{w}\|^2 = \sum_{j=1}^{J} \sum_{t=0}^{T/2^j-1} \mathbf{w}_{j,t}^2 + \mathbf{v}_{J,0}^2 = \mathbf{w}'\mathbf{w} = (\mathscr{W}\mathbf{y})'\mathscr{W}\mathbf{y} = \mathbf{y}'\mathscr{W}'\mathscr{W}\mathbf{y} = \mathbf{y}'\mathbf{y} = \sum_{t=0}^{T-1} \mathbf{y}_t^2 = \|\mathbf{y}\|^2. \tag{2.11}$$

By using this property, the energy of the original series, $\|\mathbf{y}\|^2$, is decomposed on a scale-by-scale basis.

2.2 Maximum Overlap Discrete Wavelet Transformation (MODWT)

The maximum overlap discrete wavelet transformation (MODWT) is a modified version of the DWT. As introduced above, the DWT restricts the sample size to a dyadic value T where $T = 2^J$. This restriction is relaxed by using the partial DWT, for which the sample size T should be an integer multiple of 2^{J_0} for the partial DWT of level J_0. In contrast, the MODWT of level J_0 is well defined for any sample size T.

To realize it, in contrast to the orthonormal DWT, the MODWT of level J_0 for a length T time series is a highly redundant nonorthogonal transform yielding the $J_0 + 1$ column vectors $\tilde{\mathbf{w}}_1, \tilde{\mathbf{w}}_2, \ldots, \tilde{\mathbf{w}}_{J_0}$ and $\tilde{\mathbf{v}}_{J_0}$, each of dimension T:

[5]Note that, this variance preserving property also applies to the partial DWT. As an example, for the first level partial DWT, $\mathbf{w} = \left[\mathbf{w}_1, \mathbf{v}_1\right]'$, we have $\|\mathbf{w}\|^2 = \sum_{t=0}^{T/2-1} \mathbf{w}_{1,t}^2 + \sum_{t=0}^{T/2-1} \mathbf{v}_{1,t}^2 = \|\mathbf{y}\|^2$.

$$\widetilde{\mathbf{w}} = \left[\widetilde{\mathbf{w}}_1, \widetilde{\mathbf{w}}_2, \ldots, \widetilde{\mathbf{w}}_{J_0}, \widetilde{\mathbf{v}}_{J_0}\right]', \tag{2.12}$$

where the vector $\tilde{\mathbf{w}}_j$ of length T contains the MODWT wavelet coefficients associated with changes in the original series on a scale of $\lambda_j = 2^{j-1}$, and $\tilde{\mathbf{v}}_{J_0}$ of length T contains the MODWT scaling coefficients associated with variations at scales $\lambda_{J_0} = 2^{J_0}$ and higher.

Similar to the DWT, this length $J_0 + 1$ vector of MODWT coefficients $\widetilde{\mathbf{w}}$ of level J_0 for a length T time series $\mathbf{y}$ is obtained by:

$$\widetilde{\mathbf{w}} = \widetilde{\mathscr{W}}\mathbf{y}, \tag{2.13}$$

where $\widetilde{\mathscr{W}}$ is a $(J_0+1)T \times T$ transformation matrix constructed using the MODWT filters, $\{\tilde{h}_l\}$ and $\{\tilde{g}_l\}$. These MODWT filters are a rescaled version of the DWT filters $\{h_l\}$ and $\{g_l\}$ defined above:

$$\tilde{h}_l \equiv h_l/\sqrt{2}, \quad \tilde{g}_l \equiv g_l/\sqrt{2}. \tag{2.14}$$

Therefore, as a simple example, given the Haar DWT wavelet filter and scaling filter defined above, the Haar MODWT wavelet filter and scaling filter are respectively:

$$\left\{\tilde{h}_0 = \frac{1}{2}, \tilde{h}_1 = -\frac{1}{2}\right\}. \tag{2.15}$$

and

$$\left\{\tilde{g}_0 = \frac{1}{2}, \tilde{g}_1 = \frac{1}{2}\right\}. \tag{2.16}$$

Also, in practice, the MODWT is conducted using a pyramid algorithm similar to the one for the DWT, that is, the first level wavelet and scaling coefficients for unit scale are defined as:

$$\widetilde{W}_{1,t} = \sum_{l=0}^{L-1} \widetilde{h}_l y_{t-l \bmod T} \quad \text{and} \quad \widetilde{V}_{1,t} = \sum_{l=0}^{L-1} \widetilde{g}_l y_{t-l \bmod T}, \quad t = 0, 1, \ldots, T-1, \tag{2.17}$$

And the j-th level MODWT wavelet and scaling coefficients are defined as the N dimensional vectors with elements:

$$\widetilde{W}_{j,t} = \sum_{l=0}^{L-1} \widetilde{h}_l \widetilde{V}_{j-1,t-2^{j-1}l \bmod T} \quad \text{and} \quad \widetilde{V}_{1,t} = \sum_{l=0}^{L-1} \widetilde{g}_l V_{j-1,t-2^{j-1}l \bmod T}, \quad t = 0, 1, \ldots, T-1. \tag{2.18}$$

where $j = 2, 3, \ldots, J_0$. And by keeping all vectors of wavelet coefficients and the J_0 level scaling coefficients, we get the decomposition vector as defined above: $\widetilde{\mathbf{w}} = \left[\widetilde{\mathbf{w}}_1, \widetilde{\mathbf{w}}_2, \ldots, \widetilde{\mathbf{w}}_{J_0}, \widetilde{\mathbf{v}}_{J_0}\right]'$.

Similar to the DWT, the J_0-th level MODWT is also an energy preserving transformation, that is, we have:

$$\|\mathbf{y}\|^2 = \sum_{j=1}^{J_0} \left\|\widetilde{\mathbf{w}}_j\right\|^2 + \|\widetilde{\mathbf{v}}_{J_0}\|^2 . \tag{2.19}$$

We will now briefly discuss the issue of boundary coefficients, which is a practical consideration when using the wavelet transformations introduced above.

As already explained, both the DWT and the MODWT make use of circular filtering. And a filtering operation near the beginning or end (i.e., the boundaries) of a time series (say $\{y_t\}_{t=0}^{T-1}$) treats the time series as if it were a portion of a periodic sequence with period T. While this circular filtering operation is reasonable for some series with a well chosen sample size, it can be problematic for others especially when there is a large discontinuity between y_{T-1} and y_0.

According to Percival and Walden (2000), the number of the boundary coefficients (the wavelet coefficients or scaling coefficients that are affected to any degree by the circular filtering operation) depends on the type and length of the wavelet filter (i.e., L above) and the level of the decomposition (i.e., J_0 above). Generally, the number of boundary coefficients increases when L increases and is non-decreasing as J_0 increases. A common way of dealing with the boundary coefficients is to indicate them on the plots of the wavelet or scaling coefficients and then delete them before further analysis. Since the Haar wavelet filter introduced above has a simple structure, and the number of boundary coefficients can be minimized by choosing this kind of filter (Percival and Walden, 2000), in the Monte Carlo simulations section, we will start by using the Haar wavelet filter in the MODWT decomposition.

Chapter 3

New Test for Structural Change

Let $X = \{X_t : t \in \{0, 1, \ldots, T\}\}$ be an AR(1) process such that

$$X_t = \begin{cases} \phi_0 + \phi_1 X_{t-1} + \varepsilon_t, & t \leq T^* \\ \phi_0 + \phi_2 X_{t-1} + \varepsilon_t, & t > T^* \end{cases} \tag{3.1}$$

where $\{\varepsilon_t : t \in \{1, \ldots, T\}\}$ is a sequence of independent and identically distributed (i.i.d.) normal random variables, with $E[\varepsilon_t] = 0$, and $E\left[\varepsilon_t^2\right] = \sigma^2$.[1]

We consider test for the hypothesis:

$$H_0 : \phi_1 = \phi_2, \tag{3.2}$$

against the alternative hypothesis:

$$H_1 : \phi_1 \neq \phi_2, \tag{3.3}$$

for an unknown T^* where $1 < T^* < T$.

3.1 The Test Statistic

Consider an AR(1) process X of length T with the data generating process given by equation (3.1) above. We first apply the J-th level MODWT to decompose X into $J+1$ series, each with length of T. Among these, J series are the wavelet coefficients $\left\{\tilde{\mathbf{w}}_{j,t}\right\}$ for $j = 1, 2, \ldots J$, each associated with changes on a scale of $\lambda_j = 2^{j-1}$ and another one is the scaling coefficients $\{\tilde{\mathbf{s}}_{J,t}\}$, which is associated with averages on a scale of 2^J.

[1] We conjecture that the normality assumption is not necessary for the proposed test here. However, to be consistent with the simulation setup, we add the normality assumption for the sake of rigor.

We construct the normalized partial energy sequence (NPES) based on the scaling coefficients, $\left\{\mathscr{P}_k^*\right\}_{k=1}^{\widetilde{T}_J}$.[2] Let $C_k^* = \sum_{t=1}^{k} \tilde{s}_t^2$ be the cumulative sum of squares of the scaling coefficients in the first step. Then, the NPES based on the scaling coefficients is defined as

$$\mathscr{P}_k^* = \frac{C_k^*}{C_{\widetilde{T}_J}^*} = \frac{\sum_{t=1}^{k} \tilde{s}_t^2}{\sum_{t=1}^{\widetilde{T}_J} \tilde{s}_t^2}, \qquad k = 1, 2, \ldots, \widetilde{T}_J, \tag{3.4}$$

where $\widetilde{T}_J = T - L_J + 1$ is the number of coefficients unaffected by the boundary issue we have introduced in the last section, and $L_J = \left(2^J - 1\right)(L-1) + 1$, in which L is the length of the original wavelet filter. And we define $\mathscr{P}_k^* = 0$ for $k = 0$.

Based on the wavelet transformation theory of the last chapter, the wavelet coefficients $\left\{\tilde{\mathbf{w}}_{j,t}\right\}$ for $j = 1, 2, \ldots J$ capture the behavior of X in the high frequency bands of $\left[1/2^{J+1}, 1/2^J\right]$, $\left[1/2^J, 1/2^{J-1}\right]$, $\ldots$, $[1/4, 1/2]$ respectively, while the scaling coefficients $\{\tilde{\mathbf{s}}_{J,t}\}$ capture the behavior of X in the low frequency band $\left[0, 1/2^{J+1}\right]$.

As we have demonstrated through the spectrums in the first chapter (Figure 1 of Appendix A), the proportion in which the variance at a certain frequency band contributes to the variance of an AR(1) time series depends on the autocorrelation coefficient of that series. And as this autocorrelation coefficient increases from a value close to -1 to a value close to +1, the proportion in which a certain low frequency band (say $[0, 1/2]$) contributes to the variance of the whole series increases accordingly. Therefore, under H_0, $\mathscr{P}_k^*$, the NPES based on the scaling coefficients defined in equation (3.4), should increase linearly (in a constant rate) from 0 to 1 as k increases from 0 to $\widetilde{T}_J$, while under H_1, there should be a change in the growth rate during the process when $\mathscr{P}_k^*$ increases from 0 to 1. This pattern is presented in Figures 2, 3, 4 and 5 in Appendix A.

Figure 2 and Figure 3 of Appendix A each gives three AR(1) processes of length 10,000 and 500 respectively with fixed autocorrelation coefficients of -5, 0 and 5, and their associated $\mathscr{P}_k^*$ series defined above. As we can see from the two figures, when the autocorrelation coefficient is fixed, the corresponding $\mathscr{P}_k^*$ series presents roughly a straight line. That is, it grows linearly from 0 to 1 in an approximately constant rate.

In contrast, Figure 4 of Appendix A presents two AR(1) series of length 10,000 with a structural change in the autocorrelation coefficient (from -0.5 to 0.5 (upper) and from 0.5 to -0.5 (lower), respectively) at the time of 7,000 along with their corresponding $\mathscr{P}_k^*$ series. And Figure 5 of Appendix A presents two AR(1) series of length 500 with a structural change in the autocorrelation coefficient (also from -0.5 to 0.5 (upper) and from 0.5 to -0.5 (lower), respectively) at the time of 300 along with their corresponding $\mathscr{P}_k^*$ series. These figures show that when there is a change in the autocorrelation coefficient, an inflection point appears, cutting the original line into two roughly straight pieces.

[2]This idea is illuminated by Inclan and Tiao (1994) who constructed the NPES based on the original series to detect a change in variance. By contrast, we construct the NPES based on the scaling coefficients to detect a change in the AR(1) autocorrelation coefficient.

Next, to better present the change in the structure above, we further define the centered NPES based on the scaling coefficients as

$$D_k^* = \mathscr{P}_k^* - \frac{k}{\widetilde{T}_J}, \qquad k = 1, 2, \ldots, \widetilde{T}_J, \tag{3.5}$$

with $D_0^* = D_{\widetilde{T}_J}^* = 0$ by definition. Heuristically, under H_0, the plot of D_k^* against k will oscillate around 0, while under H_1, when there is a sudden change in the autocorrelation structure, it will deviate from 0 and go out of some specified boundary with a high probability. This pattern is presented in Figure 6 of Appendix A.

Figure 6 of Appendix A shows the D_k^* series of four AR(1) series of length 500. The left two panels correspond to the series with a fixed autocorrelation coefficient of -0.5 and 0.5, respectively. The upper right panel corresponds to the case with a change of autocorrelation coefficient from -0.5 to 0.5 at the point of 300, while the lower right panel corresponds to the case with a change of autocorrelation coefficient from 0.5 to -0.5 at the point of 300. And we can see that for the cases without a structural change, the D_k^* series oscillates around 0, while the series deviate from zero significantly when there is a change in the autocorrelation coefficient creating a peak (when the coefficient changes from a higher value to a lower value) or a trough (when the coefficient changes from a lower value to a higher value) in the figure.

Finally, we do not make a difference between an increase in the autocorrelation coefficient (i.e., a trough in Figure 6-1b) and a decrease in the autocorrelation coefficient (i.e., a peak in Figure 6-2b) since what we care is the deviation of D_k^* defined above from 0, for now.[3] The desired test statistic is given by

$$D^* = \max\left(D^{*+}, D^{*-}\right), \tag{3.6}$$

where

$$D^{*+} = \max_{1 \le k \le \widetilde{T}_J} \left(\frac{k}{\widetilde{T}_J} - \mathscr{P}_k^* \right), \tag{3.7}$$

$$\text{and} \quad D^{*-} = \max_{1 \le k \le \widetilde{T}_J} \left(\mathscr{P}_k^* - \frac{k-1}{\widetilde{T}_J} \right) \tag{3.8}$$

3.2 A Feasible Version of the Test and Empirical Quantiles

The distribution of the test statistic D^* under the null hypothesis depends on several unknown parameters in the data generation process (3.1), including the constant term, ϕ_0, the standard error of the error terms, σ, and the autocorrelation under the null. In order to perform this test, we need to estimate these unknown parameters based on the given data observations.

[3]The identification of this kind of difference can be studied later

Here, we fit an AR(1) model to a given series of observations based on the Yule-Walker method to estimate the autocorrelation under the null hypothesis as well as the constant term and standard error of the error terms.[4] To be specific, the estimators of the unknown parameters in the DGP (3.1) under the null hypothesis are given by $\hat{\phi}_1 = \frac{\sum_{t=2}^{T} X_{t-1}X_t}{\sum_{t=2}^{T} X_{t-1}^2}$, $\hat{\phi}_0 = \frac{1}{T-1}\sum_{t=2}^{T}(X_t - \hat{\phi}_1 X_{t-1})$ and $\hat{\sigma}$ equals to the standard deviation of $(X_t - \hat{\phi}_1 X_{t-1})$.

Based on the estimators of the unknown parameters, we can construct a feasible version of the test statistic $\hat{D}^*$. Then, we calculate the empirical critical values of the test based on $\hat{D}^*$ from 10,000 replications.

3.3 Monte Carlo Simulations

In this section, we investigate the finite sample performance of the new test developed in this paper.

For simplicity, we start by using the Haar wavelet filter in the MODWT decomposition and choosing the decomposition level of 1.[5] Under these choices, the test statistic becomes

$$D^* = \max\left(D^{*+}, D^{*-}\right), \tag{3.9}$$

where

$$D^{*+} = \max_{1\le k\le T-1}\left(\frac{k}{T-1} - \frac{\sum_{t=1}^{k}(X_t + X_{t+1})^2}{\sum_{t=1}^{T-1}(X_t + X_{t+1})^2}\right), \tag{3.10}$$

$$\text{and} \quad D^{*-} = \max_{1\le k\le T-1}\left(\frac{\sum_{t=1}^{k}(X_t + X_{t+1})^2}{\sum_{t=1}^{T-1}(X_t + X_{t+1})^2} - \frac{k-1}{T-1}\right). \tag{3.11}$$

For the data generation process given in equation (3.1), we set: the original autocorrelation coefficient $\phi_1 = 0.1$, the sample size $T = 500$ and the change point (unknown to the testing procedure) $T^* = 300$. We restrict the constant term $\phi_0 = 1$ and the standard error of the error terms $\sigma = 2$. And we define $\delta \equiv \phi_2 - \phi_1$. Then, under the null hypothesis of no structural change (3.2), we have $\delta = 0$, while under the alternative hypothesis (3.3), we have $\delta \neq 0$. We let δ take values of $0, 0.1, 0.2, \ldots, 0.6, 0.7$, respectively, and calculate the empirical sizes and powers over 5,000 replications for the confidence levels of 1%, 5% and 10%, respectively. We compare the size and power properties of our test with the two famous CUSUM tests based on recursive residuals and OLS residuals, respectively.

[4] That is, we solve for the estimator from the Yule Walker's equations.

[5] The Haar wavelet filter has a simple structure. Besides, the number of boundary coefficients can be minimized by choosing this kind of filter (Percival and Walden, 2000).

Table 1 of Appendix B shows the empirical sizes and powers of these tests. To better present the comparison, we also plot the power curves for the D^* test and the CUSUM tests in Figure 7 of Appendix A.

The results in Table 1 and Figure 7 clearly show that the empirical sizes of the D^* test (the second column of the first panel in Table 1) are close to (but slightly larger than) the nominal sizes (i.e., 10%, 5% and 1%, respectively). And the D^* test (the 3rd to 9th columns of the first panel) has higher powers relative to the CUSUM tests based on recursive residuals (the 3rd to 9th columns of the second panel of Table 1) or OLS residuals (the 3rd to 9th columns of the third panel of Table 1).

3.4 Application to the US Inflation Rates

In this section, we apply the proposed test to the US inflation rate series. Since individuals' expectations of future inflation rates will affect the realized future inflation rates, and individuals build their expectations based on their observations of current and past inflation rates, there is serial dependence in the inflation rate series. It is of interest to investigate if its autocorrelation structure will change over time.

We get the seasonally-adjusted monthly consumer price index (CPI) data ranging from 1964 Dec. to 2010 Dec. for the United States from the FRED Economic Data Website.[6] In order to get the inflation rates, we first calculate the natural log of the CPI data and then take the first difference. The resulting monthly inflation rates from 1965 Jan. to 2010 Dec. are shown in the time series plot Figure 8 of Appendix A.

The Figure 9 of Appendix B shows the plots of the autocorrelation function (ACF) and the partial autocorrelation function (PACF) for the monthly inflation rate series, respectively. The PACF plot indicates that although the autocorrelations are significant for a large number of lags, the autocorrelations at lags 2 and above are more due to the propagation of the autocorrelation at lag 1.

Next, we apply the test developed in this thesis to identify the existence of change in the autocorrelation structure of US inflation rates for two different periods, from 1965 Jan. to 1979 Dec. and from 2001 Jan. to 2010 Dec., respectively. The results from the test are shown in Table 2 of Appendix B. The results indicate that the (first-order) autocorrelation structure for US inflation rates changed during the period from 1965 Jan. to 1979 Dec. A possible cause is that the prevalence of flexible exchange rate regimes after the Bretton-Woods system collapsed in 1973 may have affected the autocorrelation structure for the inflation rates. On the other hand, the results fail to reject the null hypothesis of no structure change for the period from 2001 Jan. to 2010 Dec. even though there was a downward fluctuation of the inflation rate level during the 2007-2008 financial crisis. Therefore, we infer that although the financial crisis caused a sudden decline of US inflation rate level, it did not change the (first-order) autocorrelation structure of the inflation rates thereafter.

[6] https://fred.stlouisfed.org/

Chapter 4

Conclusion and Discussion

In this thesis, we provide a test of structural change in the autocorrelation coefficient of an AR(1) model by constructing a test statistic of cumulative sum of squares based on a specific frequency decomposition of the variance using the maximal overlap discrete wavelet transformation (MODWT). The Monte Carlo simulation results show that the proposed test has reasonable empirical sizes and higher powers than the commonly used CUSUM tests.

Several extensions of the proposed test are possible. First, we here calculate the empirical critical values through Monte Carlo simulations. This procedure, however, can be time-consuming. It may be possible to derive the asymptotic distribution of the test statistic proposed here. Second, we investigate the test for detecting the presence of a one-time change in the autocorrelation structure. Later, this test can be extended to identify multiple changes and can even be used to locate these change points. Third, the Figure 6 of Appendix A suggests that we may be able to make a difference between an increase in the autocorrelation coefficient (i.e., a trough in Figure 6-1b) and a decrease in the autocorrelation coefficient (i.e., a peak in Figure 6-2b) using the proposed test here. Fourth, in this thesis, we restrict the discussion on a very specific data generation process–an AR(1) model. It is worth studying if the test procedure proposed here can be extended to identify the correlation structure in more general data generation process or in a general regression setting. Fifth, the proposed test here makes use of the maximal overlap discrete wavelet transformation (MODWT). The performances of this test may be affected by the choice of the specific wavelet filter, the decomposition level etc. It may be possible to find the best choice.

Bibliography

[1] Aue, A. and Horváth, L., 2013. Structural breaks in time series. *Journal of Time Series Analysis*, 34(1), pp.1-16.

[2] Bai, J., 1994. Least squares estimation of a shift in linear processes. *Journal of Time Series Analysis*, 15(5), pp.453-472.

[3] Bai, J., 1997. Estimation of a change point in multiple regression models. *Review of Economics and Statistics*, 79(4), pp.551-563.

[4] Bai, J. and Perron, P., 1998. Estimating and testing linear models with multiple structural changes. *Econometrica*, pp.47-78.

[5] Brown, R.L., Durbin, J. and Evans, J.M., 1975. Techniques for testing the constancy of regression relationships over time. *Journal of the Royal Statistical Society. Series B (Methodological)*, pp.149-192.

[6] Chow, G.C., 1960. Tests of equality between sets of coefficients in two linear regressions. *Econometrica: Journal of the Econometric Society*, pp.591-605.

[7] Fan, Y. and Gençay, R., 2010. Unit root tests with wavelets. *Econometric Theory*, 26(5), pp.1305-1331.

[8] Gençay, R., Selçuk, F. and Whitcher, B.J., 2001. *An introduction to wavelets and other filtering methods in finance and economics*. Elsevier.

[9] Gençay, R. and Signori, D., 2015. Multi-scale tests for serial correlation. *Journal of Econometrics*, 184(1), pp.62-80.

[10] Gombay, E. and Serban, D., 2009. Monitoring parameter change in AR (p) time series models. *Journal of Multivariate Analysis*, 100(4), pp.715-725.

[11] Hinkley, D.V., 1971. Inference about the change-point from cumulative sum tests. *Biometrika*, 58(3), pp.509-523.

[12] Inclan, C. and Tiao, G.C., 1994. Use of cumulative sums of squares for retrospective detection of changes of variance. *Journal of the American Statistical Association*, 89(427), pp.913-923.

[13] Li, M. and Gençay, R., 2017. Tests for serial correlation of unknown form in dynamic least squares regression with wavelets. *Economics Letters*, 155, pp.104-110.

[14] Percival, D.B. and Walden, A.T., 2000. *Wavelet methods for time series analysis*. Cambridge University Press.

[15] Perron, P., 2006. Dealing with structural breaks. *Palgrave Handbook of Econometrics*, 1(2), pp.278-352.

[16] Ploberger, W. and Krämer, W., 1992. The CUSUM test with OLS residuals. *Econometrica: Journal of the Econometric Society*, pp.271-285.

[17] Whitcher, B., Byers, S.D., Guttorp, P. and Percival, D.B., 2002. Testing for homogeneity of variance in time series: Long memory, wavelets, and the Nile River. *Water Resources Research*, 38(5).

[18] Yazgan, M.E. and Özkan, H., 2015. Detecting structural changes using wavelets. *Finance Research Letters*, 12, pp.23-37.

Appendix A

Figures

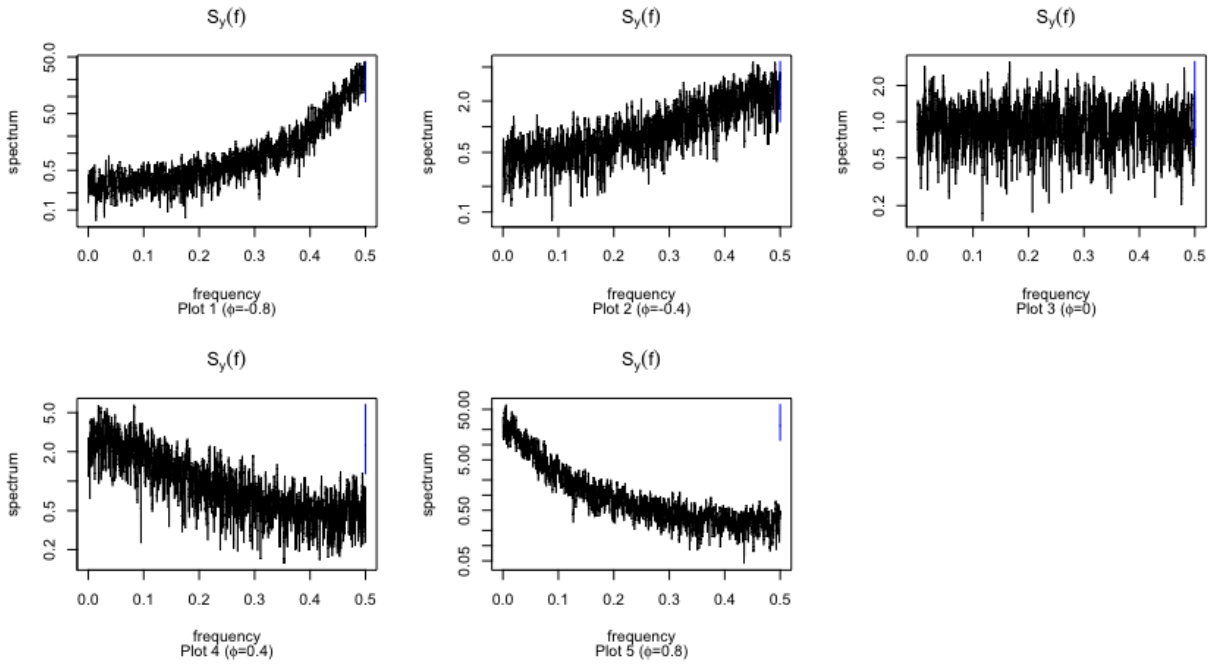

Figure 1. Spectra for AR(1) processes with different autocorrelation coefficients

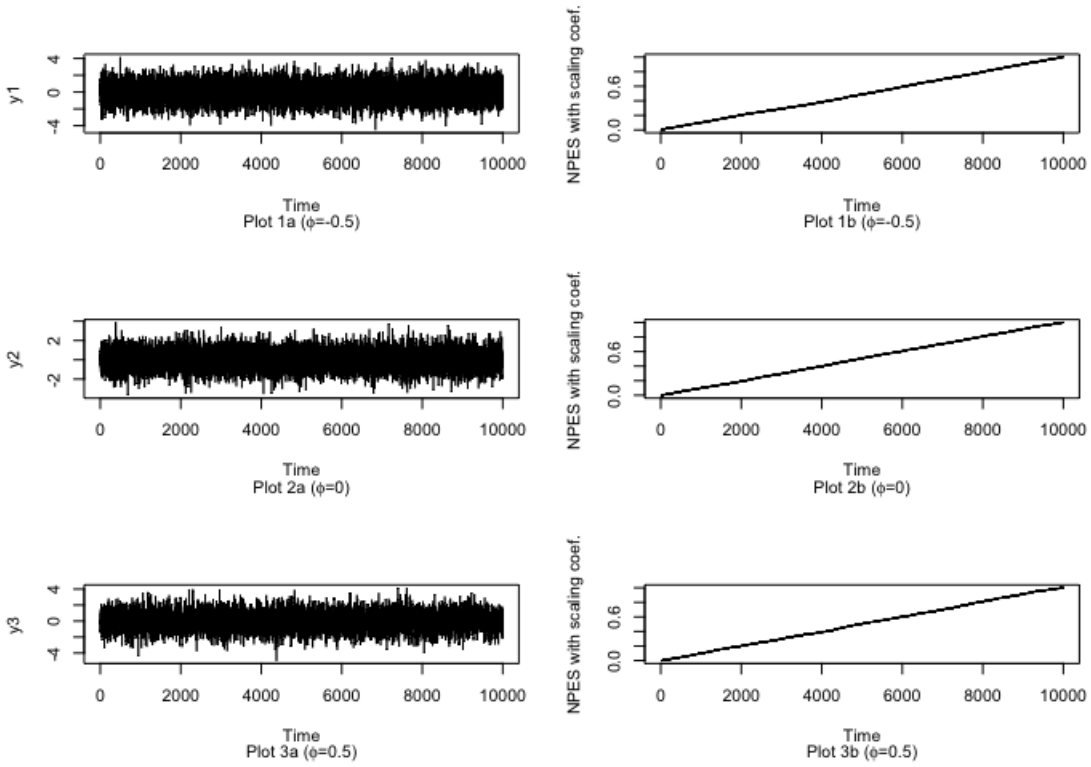

Figure 2. Examples of AR(1) processes (of length 10,000) without structural change and their corresponding $\mathscr{P}_k^*$ series

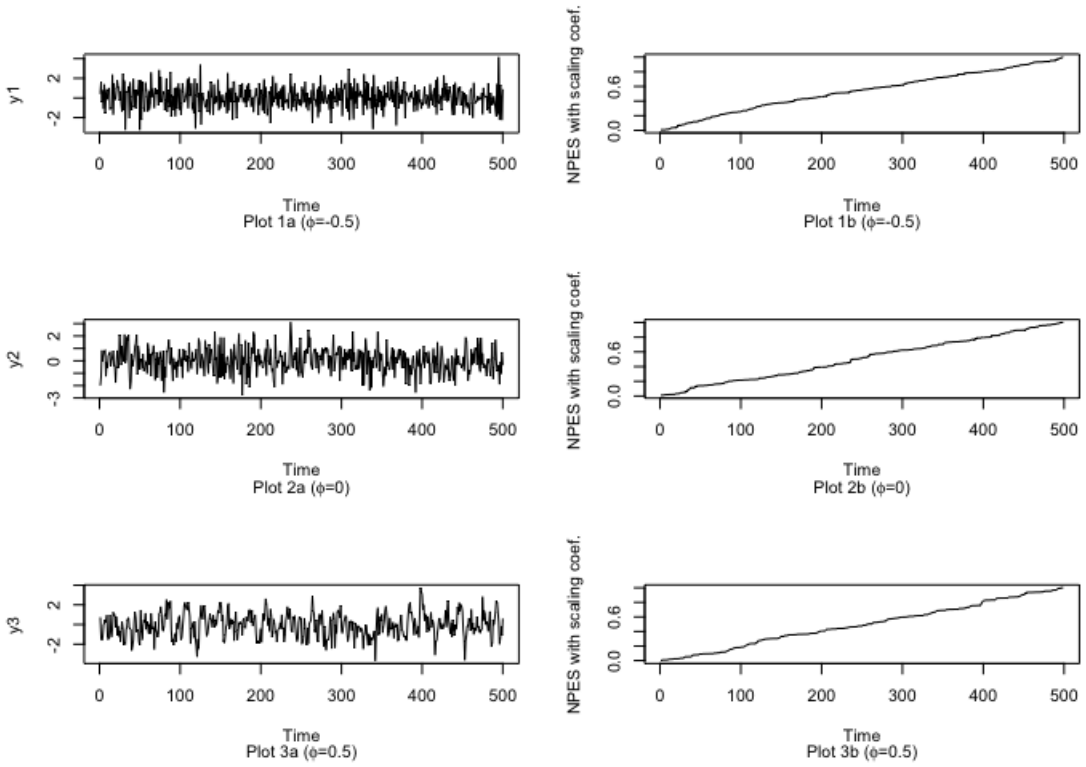

Figure 3. Examples of AR(1) processes (of length 500) without structural change and their corresponding $\mathscr{P}_k^*$ series

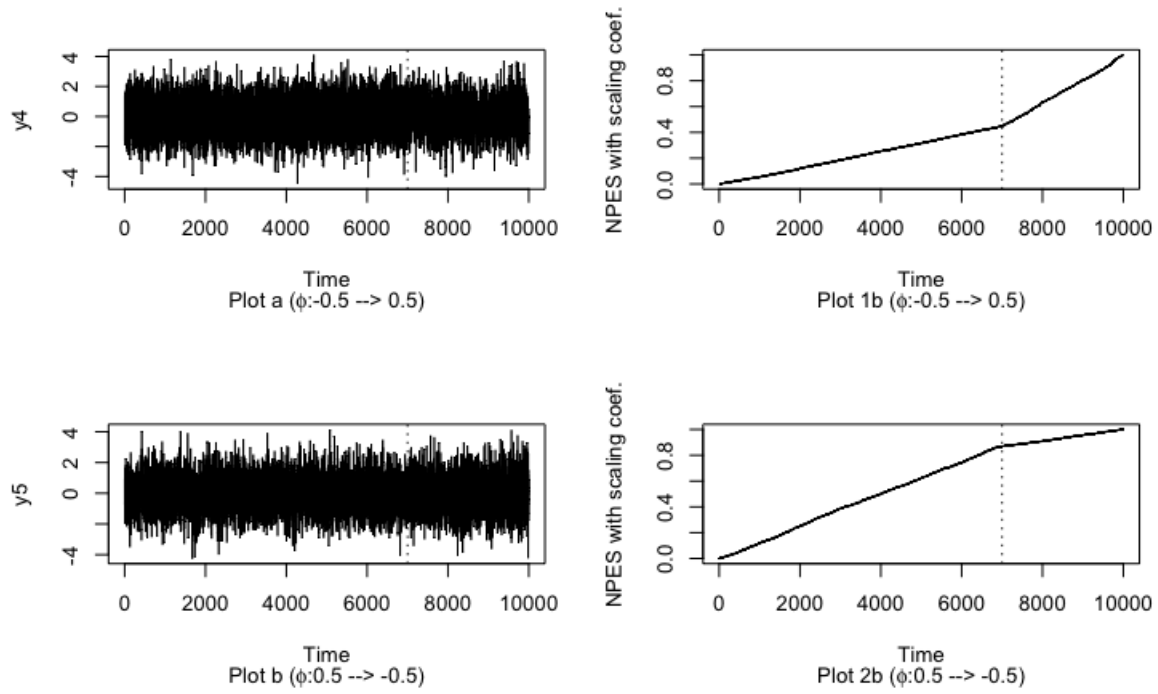

Figure 4. Examples of AR(1) processes (of length 10,000) with structural change (at time of 7,000) and their corresponding $\mathscr{P}_k^*$ series

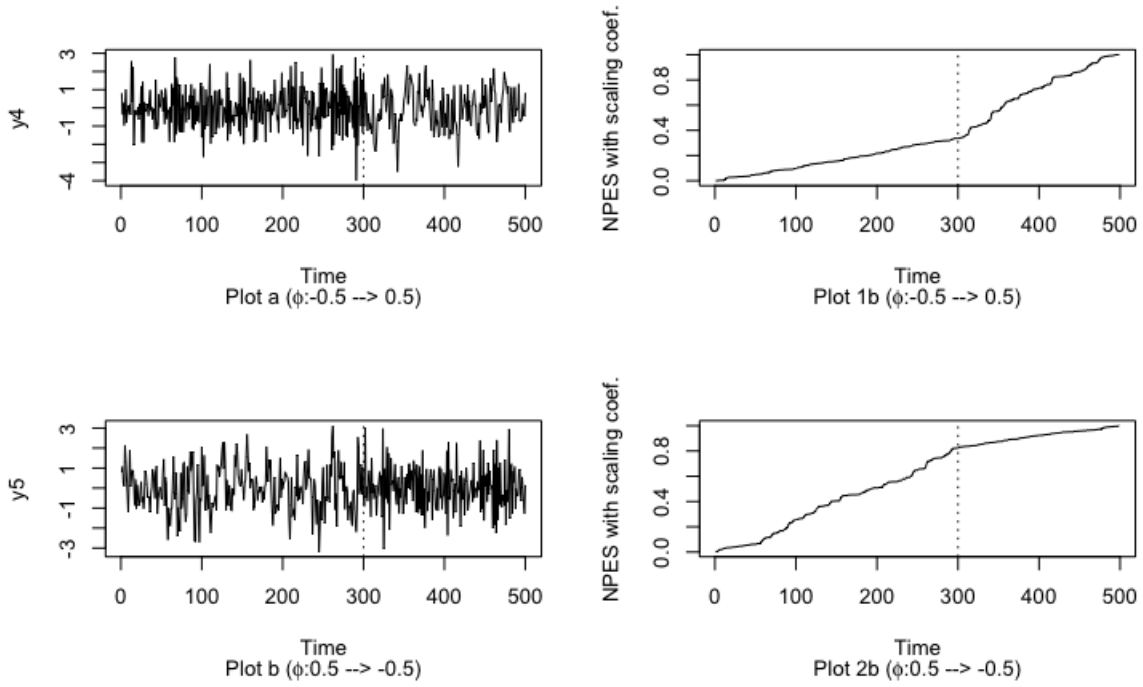

Figure 5. Examples of AR(1) processes (of length 500) with structural change (at time of 300) and their corresponding $\mathscr{P}_k^*$ series

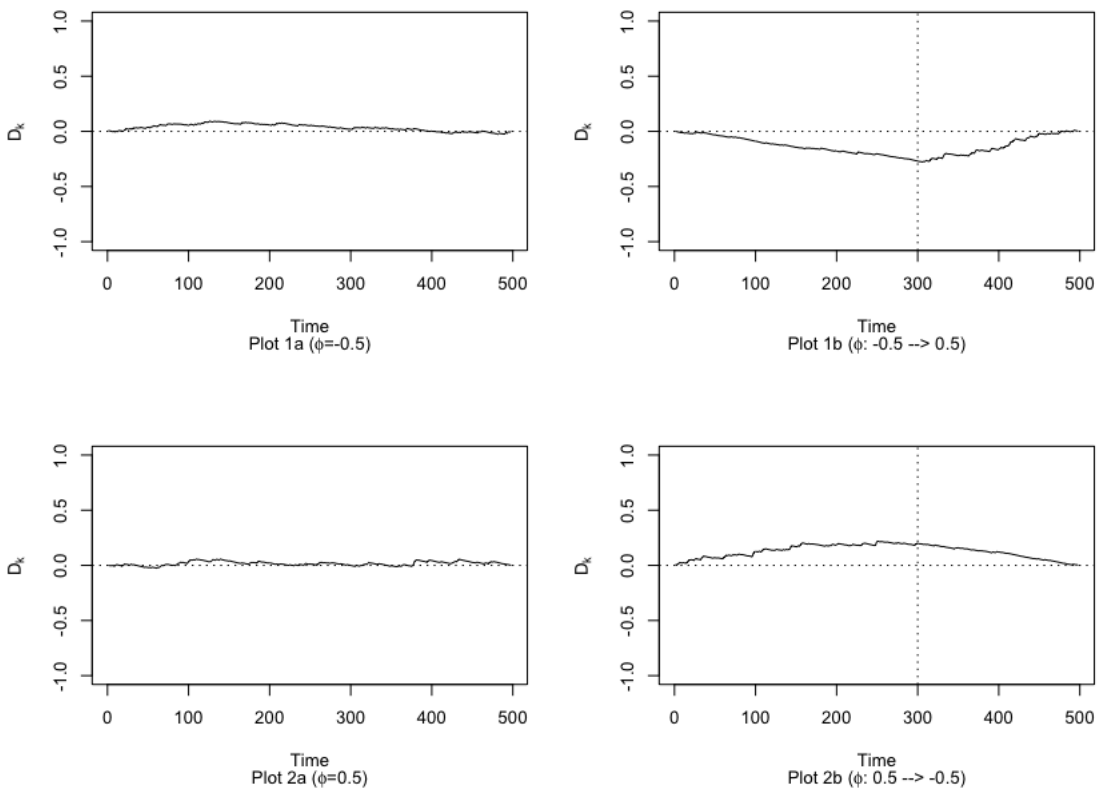

Figure 6. D_k^* series of AR(1) processes (of length 500) without(1a&2a)/with(1b&2b) structural change

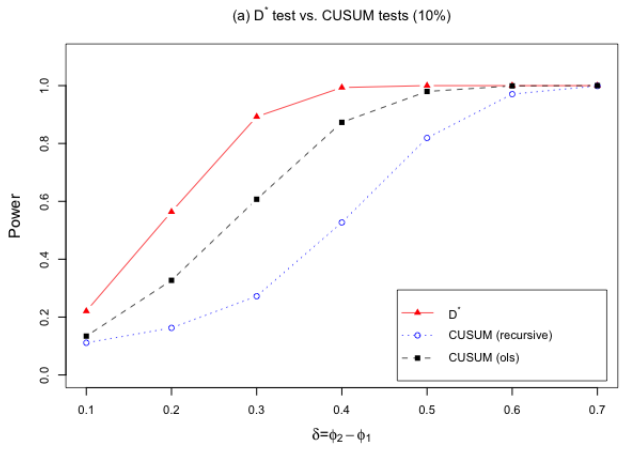

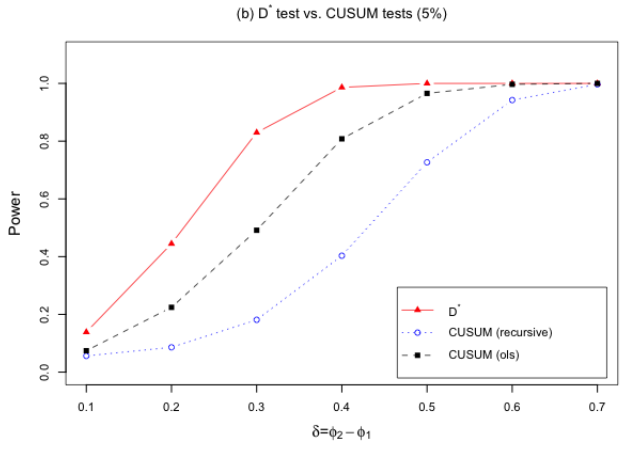

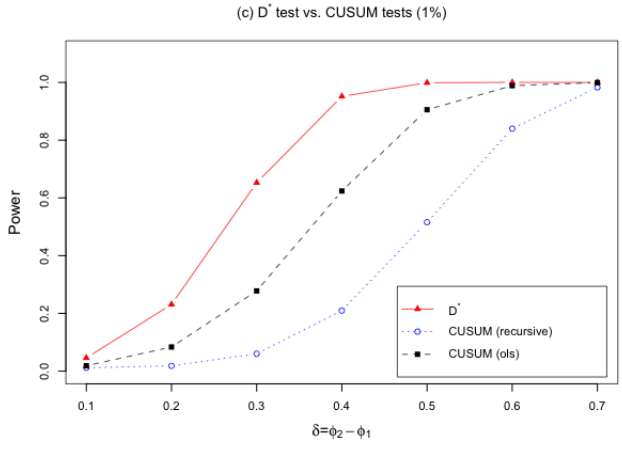

Figure 7. The power curves of the the D^* test and the CUSUM tests

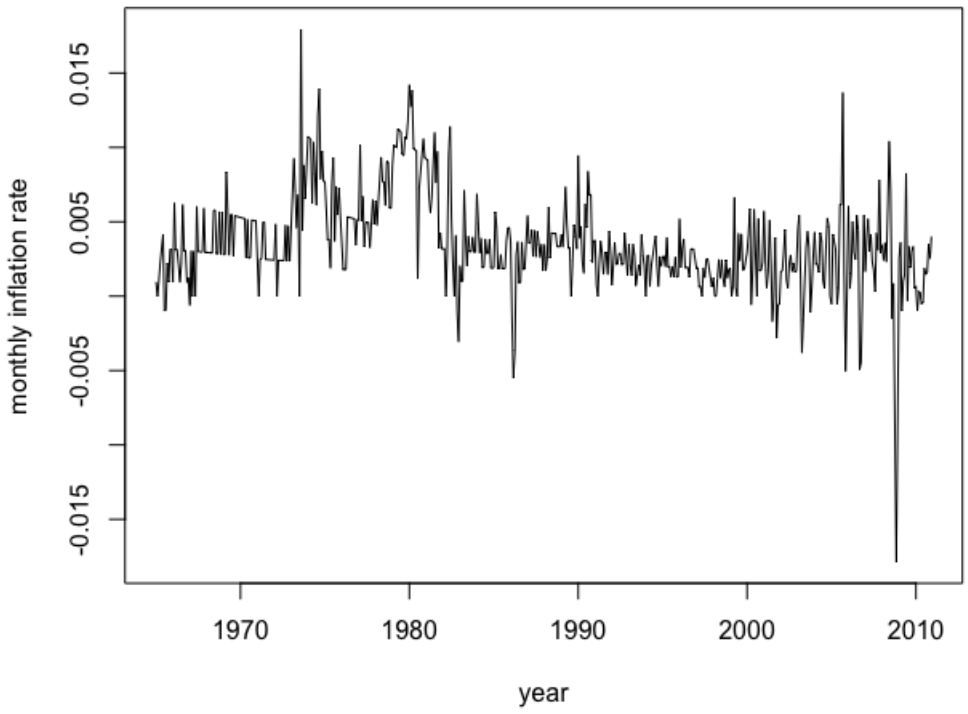

Figure 8. Monthly inflation rates for the United States

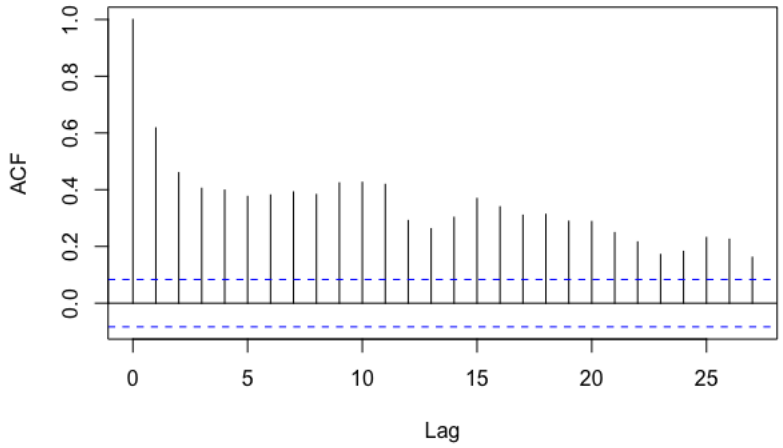

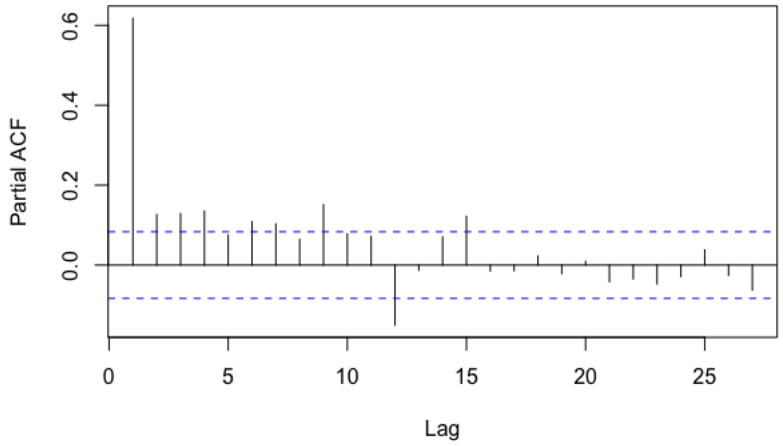

Figure 9. The ACF and the PACF of monthly inflation rates for the US

Appendix B

Tables

Table 1. Sizes and powers of the D^* test and the CUSUM tests

δ	0	0.1	0.2	0.3	0.4	0.5	0.6	0.7
				D^*				
10%	0.1047	0.2206	0.5638	0.8926	0.9934	1	1	1
5%	0.0522	0.1386	0.4448	0.8298	0.9862	1	1	1
1%	0.0105	0.0456	0.2310	0.6526	0.9516	0.9988	1	1
				CUSUM based on recursive residuals				
10%	0.0922	0.1112	0.1626	0.2722	0.5270	0.8190	0.9706	0.9990
5%	0.0452	0.0562	0.0860	0.1812	0.4032	0.7266	0.9422	0.9968
1%	0.0084	0.0118	0.0182	0.0602	0.2096	0.5156	0.8398	0.9828
				CUSUM based on OLS residuals				
10%	0.0812	0.1342	0.3270	0.6072	0.8730	0.9798	0.9990	1
5%	0.0382	0.0742	0.2244	0.4914	0.8080	0.9654	0.9968	1
1%	0.008	0.0186	0.0836	0.2778	0.6238	0.9054	0.9886	0.9992

Table 2. Results of testing change in the autocorrelation structure of the US inflation rates

Sample Period	D^* Test Statistic	10% Critical Level	5% Critical Level	1% Critical Level
1965/01-1979/12	0.3335	0.1569	0.1756	0.2160
2001/01-2010/12	0.2275	0.2312	0.2577	0.3159